Research article

Acetylcholine regulates the melanogenesis of retinal pigment epithelia cells via a cAMP-dependent pathway: A non-neuronal function of cholinergic system in retina

Ivan Kong [a,b], Gary Ka-Wing Yuen [a,b], Qi-Yun Wu [a,b], Maggie Sui-Sui Guo [a,b], Jin Gao [a,c], Tina Ting-Xia Dong [a,b], Karl Wah-Keung Tsim [a,b,*]

[a] *Division of Life Science and Centre for Chinese Medicine, The Hong Kong University of Science and Technology, Hong Kong, China*
[b] *Shenzhen Key Laboratory of Edible and Medicinal Bioresources, HKUST Shenzhen Research Institute, Shenzhen 518057, China*
[c] *Department of Neurobiology and Cellular Biology, Xuzhou Medical University, Xuzhou 221004, Jiangsu, China*

A B S T R A C T

The turnover rate of melanogenesis in retinal pigment epithelium (RPE) and its molecular signaling remain unclear. This study aimed to investigate the role of cholinergic signaling in the process of melanogenesis of cultured RPE cells. Here, a human retinal pigment epithelia cell line, ARPE-19 cell, was used to study the process of melanogenesis. The mRNA and protein expressions of cholinergic molecules, e.g., acetylcholinesterase (AChE), butyrylcholinesterase (BChE), and melanogenic molecules i.e., tyrosinase (TYR), microphthalmia-associated transcription factor (MITF), and melanin pigment were measured during melanogenesis of cultured ARPE-19 cells. Forskolin (a cAMP inducing agent), acetylcholine (ACh) and bethanechol (Bch; a muscarinic AChR agonist) were used to induce melanogenesis in the cultures. Muscarinic acetylcholine receptor (mAChR) antagonists were employed to identify the receptor subtype. During melanogenesis of ARPE-19 cells, the mRNA and protein expressions of cholinergic molecules, e.g., AChE and BChE, were increased along with melanogenic molecules, i.e., TYR, MITF and melanin pigment. Forskolin, ACh, and Bch induced an upregulation of melanogenesis in cultured ARPE-19 cultures: the induction was parallel to an increase of AChE expression. The Bch-induced enzymatic activities and mRNA levels of AChE and TYR were fully blocked by the treatments of gallamine (a M2 specific antagonist), tropicamide (a M4 specific antagonist) and atropine (non-specific antagonist for mAChRs). Cholinergic signaling via M2/M4 mAChRs regulates melanogenesis in cultured ARPE-19 cells through a cAMP-dependent pathway. This study provides insights into the regulation of RPE cell melanogenesis via a non-neuronal function of cholinergic system.

1. Introduction

Human pigment epithelia (RPE) cells are a sheet of polygonal and polarized epithelial cells that locate at the outermost layer of retina, a layer above Bruch's membrane and adjacent to photoreceptors [1]. Each RPE cell has apical processes that systematically

enwrap the outer segments of photoreceptors. This unique morphology of RPE layer provides dynamic and crucial functions in maintaining overall performances of retina, e.g., transporting nutrients from blood, excreting waste products from retina to blood circulation, and absorbing scattering light entering the eyes [2].

RPE cells contain melanin pigments in form of melanosomes. Melanin pigments play an anti-oxidative role in RPE cells protecting the cells from light-induced toxicity, cytotoxic lipid peroxidation and inflammation [3–5]. Although melanosomes are intensely packed in foetal RPE, the intensity of melanosomes is significantly dropped in aged eyes. Several lines of evidence have suggested that the turnover rates of melanin in RPE cells are different in younger and older individuals. The lack of melanin, or failure in turning over, in adult RPE layer could lead to development of age-related macular degeneration (AMD), one of the leading causes of blindness in the world today [6–9]. In patients diagnosed with AMD, there were observations of different severity of melanin disruption in the captured multi-spectral images [8]. By providing melanin-liked biomaterial to RPE, the applied material was shown to counteract the oxidative stress, as induced by reactive oxygen species (ROS) [10]. In an *in vitro* study, artificially pigmented RPE cells demonstrated a significant attenuation of ROS damage, as induced by the exposure to blue light, which indicated that melanin could serve as both physical and biochemical protective agent to RPE cells [11]. Melanogenesis has been well-documented in skin epidermal layer [12–14]. The exposure to UV is the main cause of melanin production in skin [6–9], which is mediated by α-melanocyte-stimulating hormone (MSH) released from keratinocytes and then acting on melanocytes to induce the release of melanin [15,16]. The released melanin is being taken up by keratinocytes, and in turn, the skin is darkened in response to sunlight exposure. In addition, the role of acetylcholine (ACh) in triggering the process of melanogenesis in skin has been proposed [14]. The expressions of various cholinergic molecules have been identified in keratinocytes and melanocytes of skin epidermal layer [17–19]. The concept of a "skin synapse" has been proposed by interplay of keratinocytes and melanocytes in directing the solar light-induced melanogenesis via the action of ACh [14]. ACh is being synthesized and released by keratinocytes: the release is triggered by light-activated opsin. The released ACh binds onto muscarinic acetylcholine receptor (mAChR) of melanocyte, as such to regulate melanogenesis.

Here, we provide several lines of evidence to support the cholinergic functions, as well as signalling mechanism, in regulating melanogenesis of RPE cells. ARPE-19 cells, a spontaneous arising human RPE cell line, was employed here to reveal the expressions of cholinergic molecules, as well as to demonstrate the cholinergic system in regulating the melanogenesis process in RPE. Our results provide a new insight on the understanding of melanogenesis in RPE through *In vitro* models, as well as to provide possible preventions of age-related macular degeneration (AMD) through different aspects of melanogenesis.

2. Materials and methods

2.1. Materials

Dulbecco's modified Eagle medium (DMEM), fetal bovine serum (FBS) and other reagents for cell culture were purchased from Thermo Fisher Scientific (Waltham, MA). Antibodies were purchased from Santa Cruz Biotechnology (Santa Cruz, CA), Thermo Fisher Scientific and Cell Signaling Technology (Beverly, MA). RNAzol ® RT reagent, melanin, acetylcholine iodide (A7000), forskolin (F3917), H-89 dihydrochloride hydrate (B1427), tetra-iso-propylpyrophos-phoramide (iso-OMPA), 5,5-dithiobis-2-nitrobenzoic acid, L-dopa, dimethyl sulfoxide (DMSO) and other chemicals were purchased from Sigma-Aldrich (St. Louis, MO).

2.2. Cell Culture

Human retinal pigment epithelia (RPE) cell line, ARPE-19 (CRL-2302), and A375 human melanoma cell line (CRL-1619) were from American Type Culture Collection (ATCC; Manassas, VA). The cells were cultured in DMEM culture medium supplemented with 10 % foetal bovine serum (FBS) in 37 °C incubator supplied with 5 % CO_2. The passage number of ARPE-19 cells was kept from 10 to 20 throughout the entire study. The cell density of cultures was determined by using cell counting method with hemocytometer, and the initial seeded cell number was 2×10^4.

2.3. Enzymatic assay

AChE activity was measured by Ellman's assay [20,21] with additional 0.1 mM of tetra-iso-propylpyrophosphoramide (iso-OMPA, Sigma-Aldrich) for 15 min under 37 °C incubation prior to the assay's reaction. Fifty μL of cell lysate was added with 0.625 mM of acetylthiocholine iodide and 0.5 mM of 5,5-dithiobis-2-nitrobenzoic acid with 80 μL of 80 mM of Na_2HPO_4 buffer. The absorbance was read at 405 nm alongside with recorded time of reaction. For tyrosinase (TYR), 20 μL of 0.1 M of 1 x phosphate buffered saline (PBS, pH 7) was added to each well. Then, 80 μL of 10 μM of L-dopa was added to 50 μL of cell lysate in each well of a 96-well plate to initiate the reaction. The 96-well plate was incubated at 37 °C for the entire reaction. The absorbance was read at 405 nm.

2.4. Measurement of melanin

Cultured ARPE-19 cells were collected via trypsinization from 100-mm cell culture dish in 1.5 mL Eppendorf tubes and centrifuged with 15,000 rpm for 15 min to collect the cell pellets. The cell pellets were then supplemented with 150 μL of 1M NaOH with 10 % dimethyl sulfoxide (DMSO) and heated for 1 h under 90 °C. The absorbance was read at 470 nm.
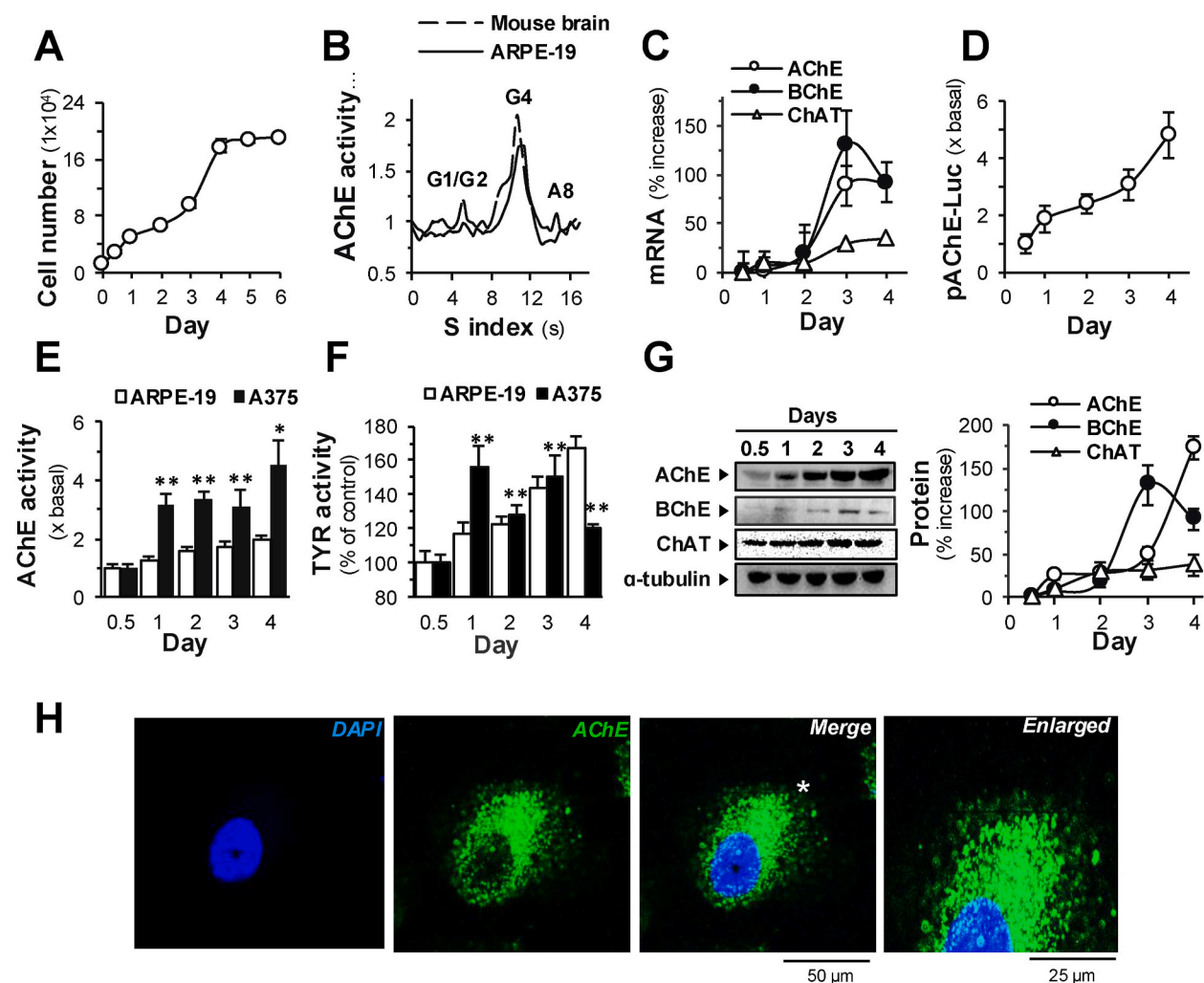
Fig. 1. Expression of cholinergic molecules and TYR in cultured ARPE-19 cells.
(**A**) Cell number of cultured ARPE-19 cells was determined by cell counting. (**B**) Cultured ARPE-19 cell, or mouse brain, lysates (200 μL) were subjected to sucrose gradient density analysis. AChE activity was plotted as a function of the sedimentation (*S*) value, estimated from the position of the sedimentation markers. (**C**) The mRNA levels of AChE, BChE and ChAT in cultured ARPE-19 cells were quantified by RT-qPCR. GAPDH was used as reference gene. (**D**) ARPE-19 cells were transfected with pAChE-Luc, and luciferase assay was performed. (**E**) The enzymatic activity of AChE, or (**F**) TYR, in cultured ARPE-19 and A375 cells. (**G**) Cell lysates (~40 μg) were collected for Western blotting of AChE (~75 kDa), BChE (~95 kDa), ChAT (~65 kDa) in cultured ARPE-19 cells, and α-tubulin (~55 kDa) was a loading control. (**H**) Immunofluorescent staining of anti-AChE (green) and nucleus (blue) in ARPE-19 cells with permeabilization with 0.1 % Triton X-100. Values were mean ± SEM., $n = 4$, each with triplicate samples. $^*p < 0.05$; $^{**}p < 0.01$, $^{***}p < 0.001$.

2.5. Sucrose density gradient analysis

Different molecular isoforms of AChE were analysed by sucrose density gradient method. The protein samples were mixed with alkaline phosphatase and β-galactosidase in a 12-mL centrifugation tube, and a series of 5 %–20 % sucrose solution in low salt lysis buffer was prepared. The sucrose gradient mixture was gently layered one after the other by FC 203B Fraction Collector (Gilson, Middleton, WI), and the tubes with the protein samples were centrifuged at 4 °C for 16 h at 38,000 rpm in SW41 Ti rotor (Beckman, Palo Alto, CA) and ultracentrifuge (CP80WX, Hitachi, Hitachinaka, Japan). Around 42 fractions were collected and assayed for activities of AChE, β-galactosidase and alkaline phosphatase.

2.6. SDS-PAGE and Western blot

Total cell protein lysate was obtained by using RIPA-buffer (150 mM NaCl, 50 mM Tris pH 8.0, 10 % sodium deoxycholate, 10 % SDS and 1 % Nonident P-40) with protease inhibitor cocktail that consisted of 10 μM leupeptin, 5 μM benzamidine hydrochloride, and 10 mM aprotinin. The aliquots of the cell lysates were then shaken for 15 min at 4 °C and centrifuged for 10 min at 12,000 g. The
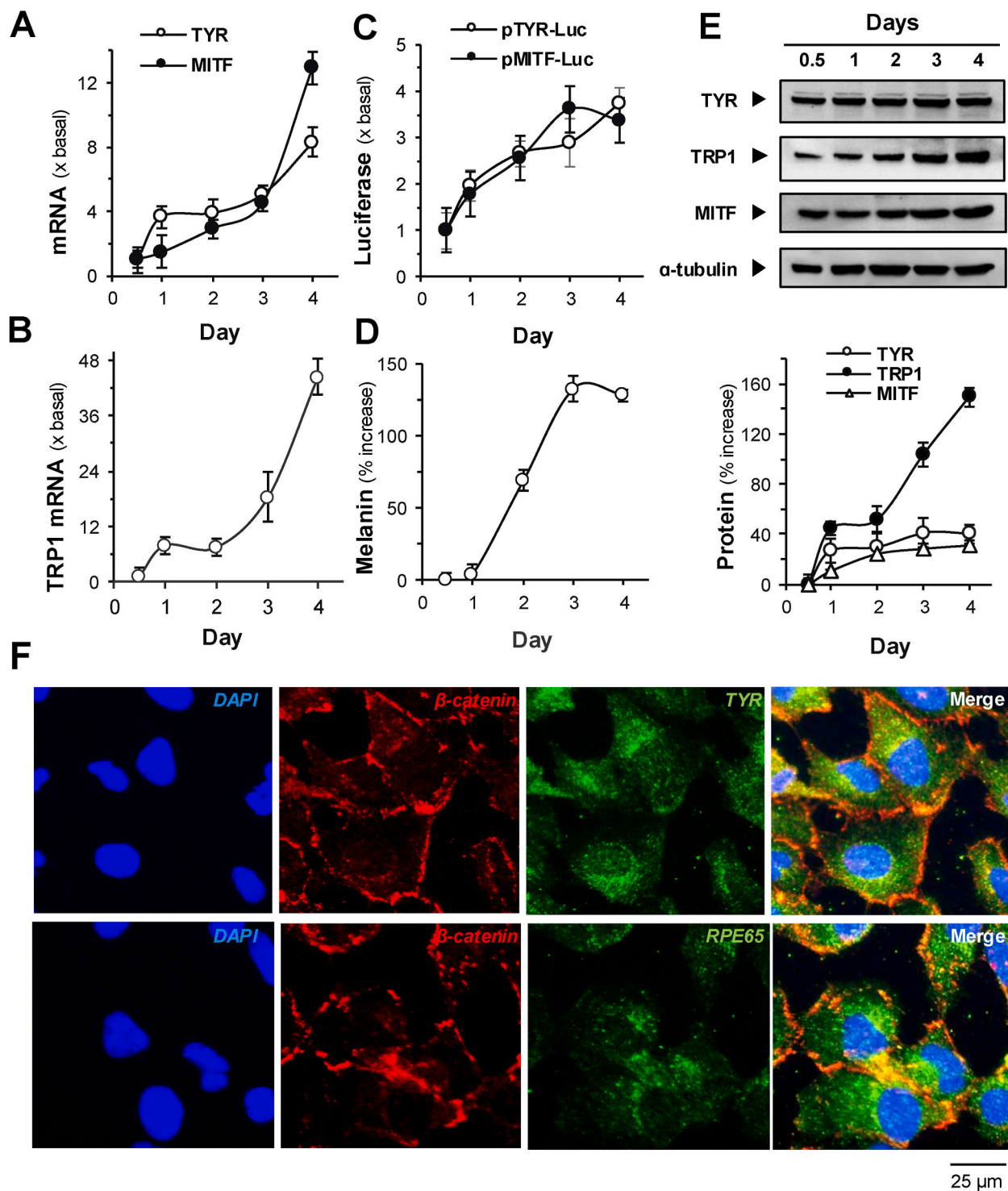
Fig. 2. Expression and localization of melanogenic molecules in ARPE-19 cells. (**A-B**) The mRNA levels of TYR, MITF and TRP1 in cultured ARPE-19 cells were determined by RT-qPCR. GAPDH was used as a reference gene. (**C**) ARPE-19 cells were transfected with pTYR-Luc and pMITF-Luc, and then luciferase was measured. (**D**) Amount of melanin in cultured ARPE-19 cells was determined. (**E**) Cell lysates (~40 μg) were collected for Western blotting of melanogenic proteins, i.e., TYR (~85 kDa), TRP1 (~80 kDa), MITF (~55 kDa) in cultured ARPE-19 cells, and α-tubulin (~55 kDa) was used as a loading control. (**F**) The staining of anti-TYR (green), anti-retinal pigment epithelium-specific 65 kDa protein (RPE65) (green), β-catenin (red) with permeabilization with 0.1 % Triton X-100. Nucleus were stained with DAPI. Values were mean ± SEM., *n* = 4, each with triplicate samples.
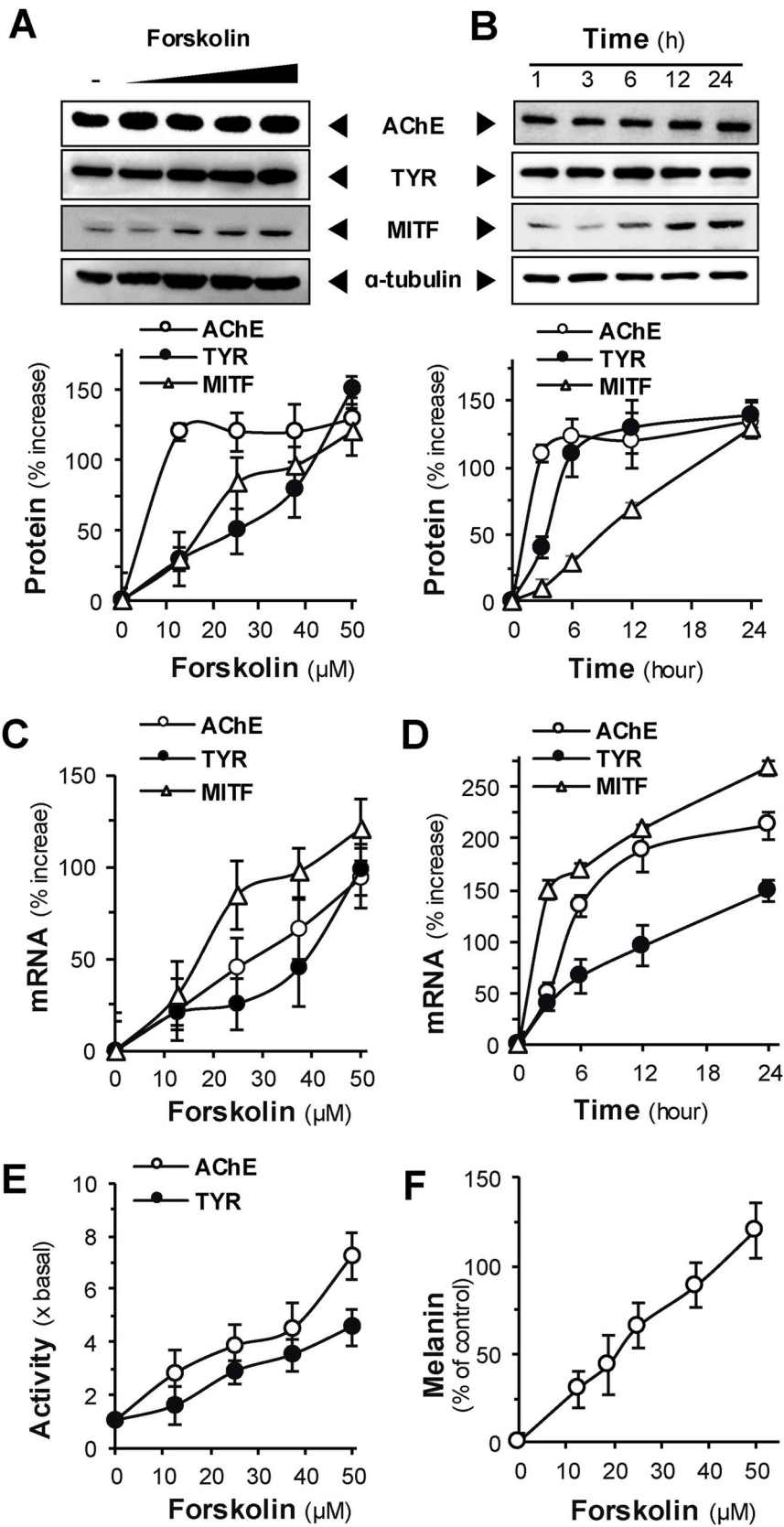
(caption on next page)

Fig. 3. Forskolin regulates melanogenic molecules and AChE. (**A**) Forskolin (0–50 μM) was applied in cultured ARPE-19 cells for 24 h before the Western blot analysis. AChE (~75 kDa), TYR (~85 kDa), MITF (~55 kDa) and α-tubulin (~55 kDa) were revealed and qualified. (**B**) Forskolin (50 μM), as in (A), was applied and cell lysates (~40 μg) were collected by different hours. (**C-D**) The mRNA levels of AChE, TYR and MITF in cultured ARPE-19 cells were quantified by RT-qPCR. GAPDH was used as a reference gene. (**E**) Cell lysates (~40 μg) were collected. The enzymatic activities of AChE and TYR were determined. (**F**) Melanin contents in cultured ARPE-19 cells was determined by boiling ARPE-19 cell lysates with 1M NaOH for 1 h and the absorbance was read at 490 nm. Values were mean ± SEM., $n = 4$, each with triplicate samples.

supernatant was isolated and normalised to 50 μg of protein. The protein was then loaded onto 8–10 % sodium dodecyl sulfate (SDS)-polyacrylamide gels (SDS-PAGE) and transferred to nitrocellulose membrane. The membrane was blocked with 5 % skimmed milk for 1 h in room temperature and incubated with primary antibody that included anti-AChE 1:1,000, anti-BChE 1:1,000, anti-choline acetyltransferase (ChAT) 1:1,000, anti-MITF 1:800, anti-tyrosinase related protein-1 (TRP1) 1:1,000, anti-α tubulin 1:2000 (Santa Cruz Biotech, Santa Cruz, CA) and anti-TYR 1:800 (Thermo Fisher Scientific, Waltham, MA) in 5 % bovine serum albumin (BSA) for 16 h in 4 °C. The immune-reactive protein bands were visualized by enhanced chemiluminescence (ECL) western blotting detection kit (Thermo Fisher Scientific). The bands intensities were analysed via Chemidoc Imaging system (Bio-Rad Laboratories, Hercules, CA).

2.7. RT-PCR and qPCR analysis

Total RNA was isolated as per the manufacturer's protocol of RNAzol® reagent (Molecular Research Center, Cincinnati, OH). The total RNA was precipitated with absolute isopropanol and washed with 75 % (v/v) ethanol and eluted with RNAase free water. The RNA quality was determined by Nanodrop™ to the nearest ratio of ~2.0. RT-PCR was performed as per manufacturer's protocol of 5x PrimeScript RT Master Mix (Takara, Shiga, Japan), where 500 ng/μL of RNA was used to generate cDNA. The specific primer sequences
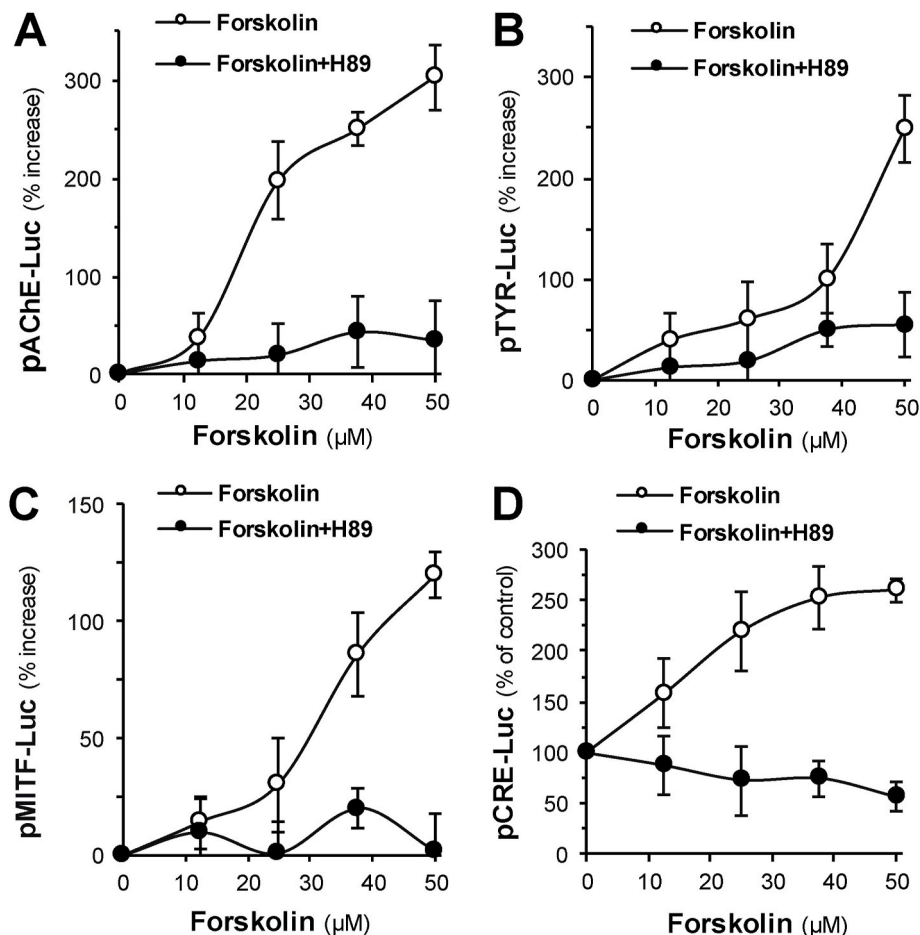

Fig. 4. Forskolin promotes melanogenesis via a cAMP-dependent pathway.
Cultured ARPE-19 cells were transfected with DNA constructs contained luciferase driven by the promoters, (**A**) pAChE-Luc, (**B**) pTYR-Luc, (**C**) pMITF-Luc and (**D**) pCRE-Luc, then the transfected cells were treated with forskolin with or without H89 (5 μM). Cell lysates were collected after 24 h of incubation, followed by luciferase assay. Values were mean ± SEM., $n = 4$, each with triplicate samples.
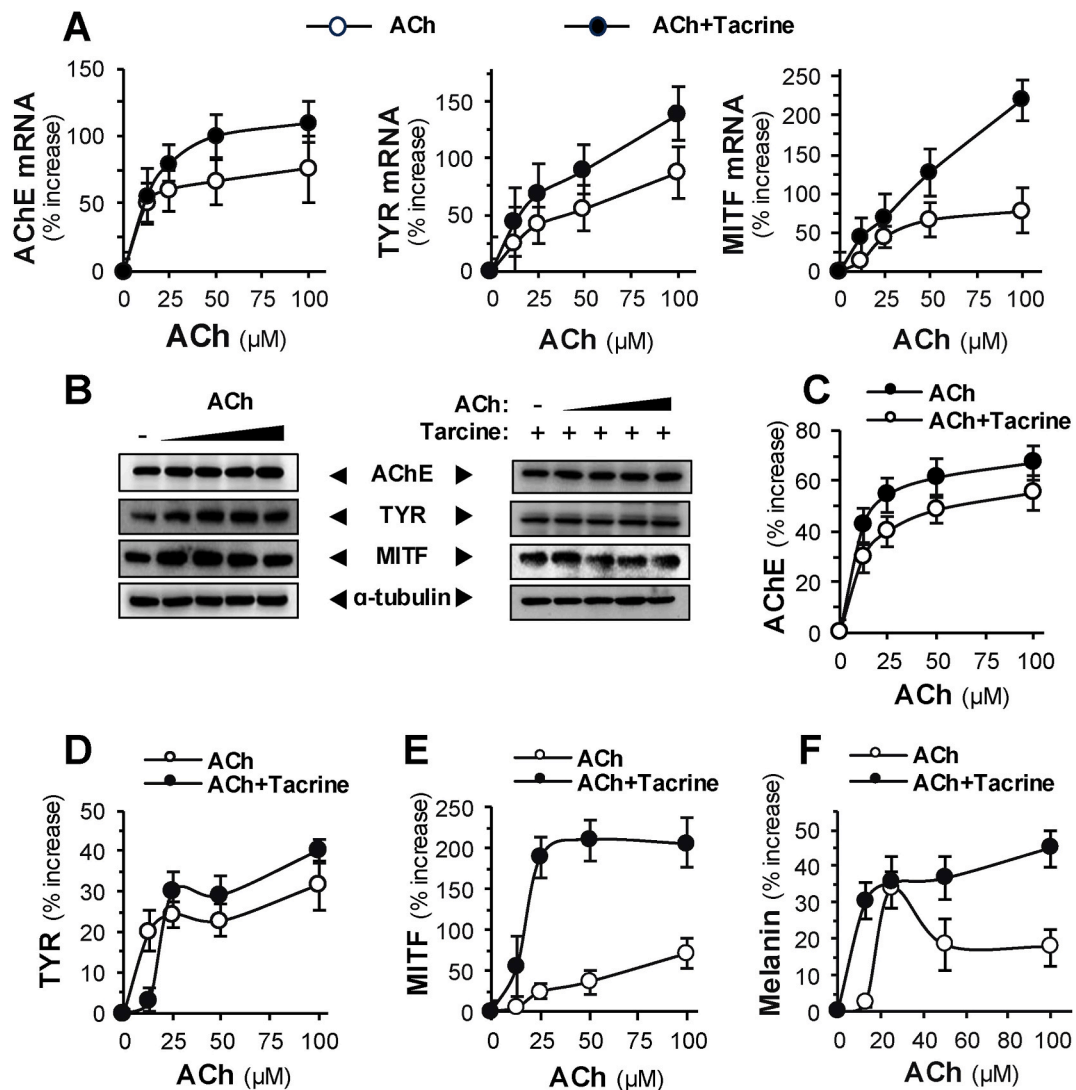
Fig. 5. ACh regulates expressions of melanogenic molecules and AChE.
Cultured ARPE-19 cells were treated with 0–100 μM of ACh with or without tacrine (5 μM). (**A**) The mRNA levels of AChE, TYR and MITF in cultures were quantified by RT-qPCR. GAPDH was used as a reference gene. (**B**) Cell lysates (~40 μg) were collected. Western blot analysis was employed to determine the protein levels of AChE (~75 kDa), TYR (~85 kDa), MITF (~55 kDa), and α-tubulin (~55 kDa) was used as a loading control. The treatment was as in (A). Qualification of protein levels of (**C**) AChE, (**D**) TYR, and (**E**) MITF. (**F**) Melanin content was determined. Values were mean ± SEM., $n = 4$, each with triplicate samples.

were sense 5′- GTT CTC CTT CGT GCC TGT GGT A-3′, antisense 5′-ATA CGA GCC CTC ATC CTT CAC C for human AChE, sense 5′- CGT GCT CAA CAA TGT CGA TTC TG-3′, antisense 5′- GTC CAT CAT GTA ATT GTT CCA GCG-3′ for human BChE, sense 5′-GTG GCT CAG AAC AGC AGC ATC A-3′, antisense 5′-CCT CAC TGA GAC GGC GGA AAT T-3′ for human ChAT, sense 5′- AGC ACC CCA CAA ATC CTA ACT TA-3′, antisense 5′- ATG GCT GTT GTA CTC CTC CAA TC-3′ for human TYR, sense 5′-GTA ACA GCA CCG AGG ATG G-3′, antisense 5′- TCC AAG CAC TGA GCG ACA T-3′ for human TRP1, sense 5′-TGA ATC GGA TCA TCA AGC AA-3′, antisense 5′- CGC TAA CAA GTG TGC TCC GTC-3′ for human MITF, sense 5′-CCA CTC CTC CAC CTT TGA CG-3′, antisense, 5′-CCA CCA CCC TGT TGC TGT AG-3′ for human glyceraldehyde 3-phosphate dehydrogenase (GAPDH). The following conditions were employed in Roche 480 Lightcycler (Roche, Basel, Switzerland) for the entire qPCR, amplification for 45 cycles. Each cycle included 95 °C of denaturation for 30 s, 55 °C annealing for 30 s and extension at 72 °C extension for 20 s.

2.8. Fluorescent immunostaining

In brief, cultured ARPE-19 cells were seeded on coverslip coated with poly-D-lysine (Thermo Fisher Scientific) and washed with 1x PBS. Then, the cells were fixed with 4 % paraformaldehyde (PFA) for 15 min in room temperature and followed by blocking with 5 %
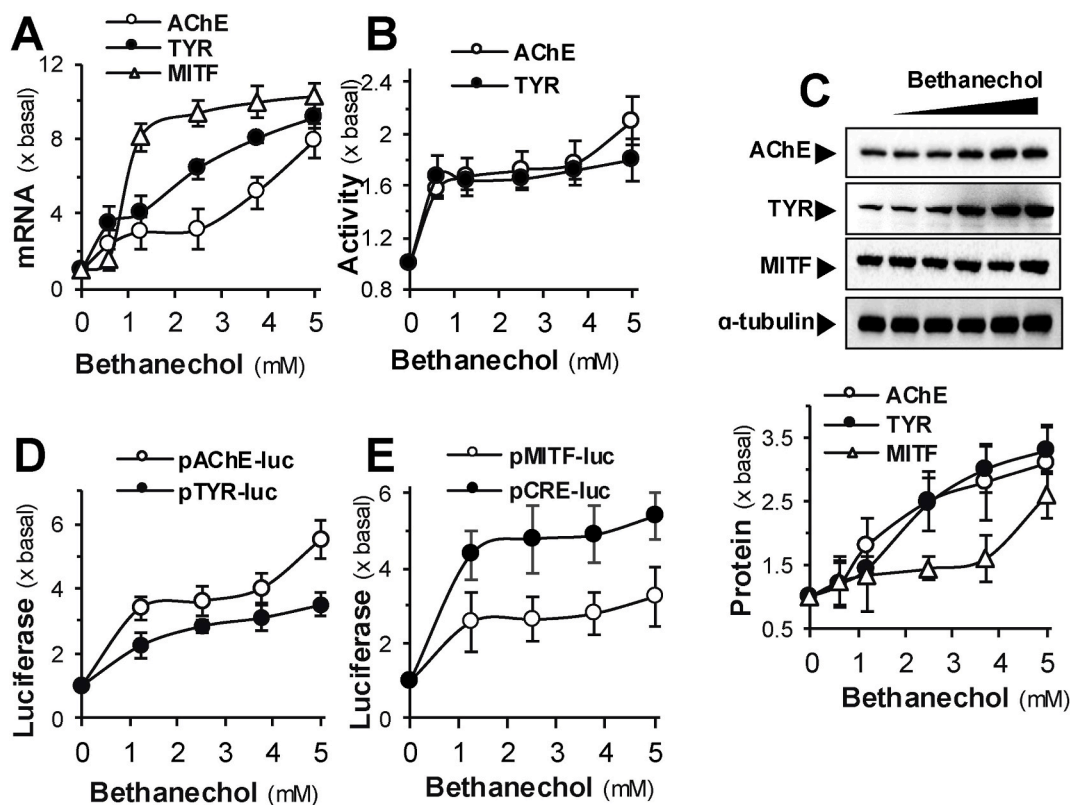
Fig. 6. Bethanechol upregulates melanogenesis and expression of AChE.
Cultured ARPE-19 cells were treated with 0–5 mM of bethanechol (**A**) The mRNA levels of AChE, TYR and MITF in cultures were quantified by RT-qPCR. GAPDH was used as a reference gene. (**B**) Cell lysates (~40 μg) were collected. Enzymatic assays were determined. (**C**) Cell lysates (~40 μg) were collected for Western blotting of AChE (~75 kDa), TYR (~85 kDa), MITF (~55 kDa) in cultures, and α-tubulin (~55 kDa) was used as a loading control (upper panel). Qualification was shown in the lower panel. (**D-E**) Cultured ARPE-19 cells were transfected with the promoter constructs, pAChE-Luc, pTYR-Luc, pMITF-Luc and pCRE-Luc. Cell lysates were collected after 24 h of incubation, followed by luciferase assay. Values were mean ± SEM., *n* = 4, each with triplicate samples.

BSA. The cells were permeabilised with 0.1 % Triton X-100 in 1 x PBS for 15 min. The fixed cells were incubated over-night at 4 °C with primary antibody (or without for controls), anti-mouse AChE antibody (A-11, Santa-Cruz) 1:200, anti-mouse TYR antibody (T311, Thermo Fisher Scientific) 1:200, anti-mouse β-catenin (SC-7963, Santa Cruz) 1:200, anti-rabbit RPE65 (Abclonal, Woburn, MA) 1:200, anti-mouse M2 mAChR (ab2805, Abcam, Cambridge, UK) 1:200, anti-rabbit M4 mAChR (ab189432, Abcam) 1:200. The secondary antibodies (1:200), goat anti-mouse IgG Alexa Fluor 488, goat anti-rabbit IgG Alexa Fluor 488, Goat anti-mouse IgG Alexa Fluor 647 and goat anti-rabbit IgG Alexa Fluor 647 were treated for 1 h, room temperature. The cover slips were then mounted with ProLong® Gold Antifade Reagent with DAPI (Cell Signalling Technology, Danvers, MA).

2.9. Luciferase assay

Details of luciferase assay were performed as per described in Siow et al. [22]. In brief, the cells were lysed with 1X passive lysis buffer diluted from 5X stock, and the luciferase excitatory activity was detected by luciferase assay system (Promega, Madison, WI). The expression levels of the target genes were compared with untreated groups.

2.10. Statistics

The presented data were expressed as mean ± SD. Statistics comparison analysis of means between different treatment groups were analysed by using one-way ANOVA followed by a Bonferroni post-hoc test. Significant values were represented as *$p < 0.05$, **$p < 0.01$, ***$p < 0.001$.
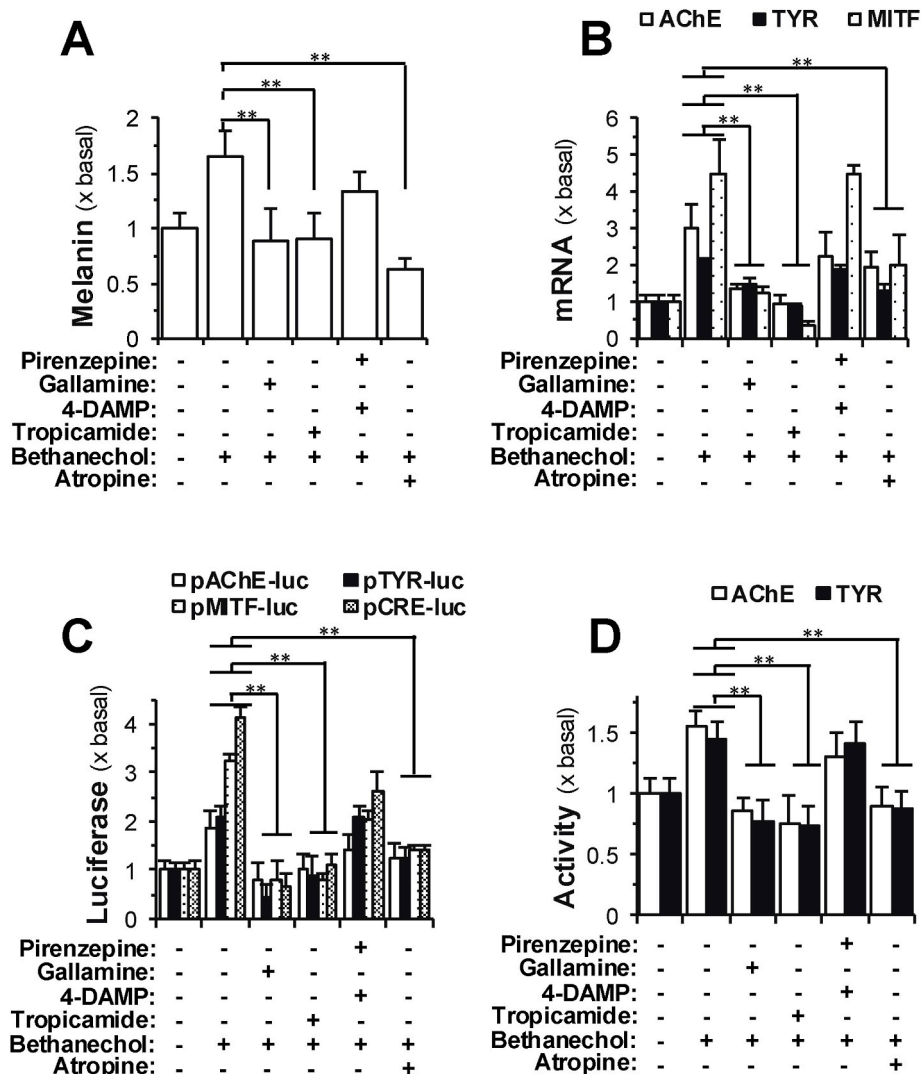
Fig. 7. The ACh-induced melanogenesis and expression of AChE are mediated by M2 and M4 mAChRs.
Specific mAChR antagonists were used to inhibit the effect of bethanechol (a non-specific agonist of mAChRs, 5 μM). The corresponding specific antagonists to mAChRs are pirenzepine (M1 mAChR, 10 μM), gallamine (M2 mAChR, 10 μM), 4-DAMP (M3 mAChR, 10 μM), tropicamide (M4 mAChR, 10 μM), and atropine (non-specific antagonist to all mAChRs, 20 μM). (**A**) The content of melanin contents, (**B**) the mRNA levels of AChE, TYR and MITF having GAPDH as a reference gene, (**C**) the activities of luciferase driven by promoters, pAChE-Luc, pTYR-Luc, pMITF-Luc and pCRE-Luc, (**D**) the enzymatic activities of cell lysates (~40 μg) corresponding to AChE and TYR. +, drug applied and -, drug not applied. Values were mean ± SEM., $n = 4$, each with triplicate samples. $*p < 0.05$; $**p < 0.01$, $***p < 0.001$.

3. Results

3.1. Regulation of cholinergic molecules during melanogenesis

ARPE-19 cells at 2×10^5 density were cultured, and the number (~18×10^5) reached the plateau on day 4 (Fig. 1A). After 4 days of culture, cell death was revealed, and therefore the analysis was mostly done within 4 days. By sucrose density gradient analysis, the detected molecular forms of AChE were G1, G2, G4 and A8: the major form was G4 (Fig. 1B). The G1, G2 and A8 forms were at minimal detection. RT-qPCR analyses of AChE, BChE and ChAT in the cultures showed upregulation of the mRNA expressions in time-dependent manners. The mRNA level of AChE started to plateau on day 3 (~90 % of increase); while BChE (~130 % of increase) and ChAT (~30 % of increase) mRNAs were at peak on day 3 (Fig. 1C). The luciferase activity driven by the *ACHE* promoter in pAChE-Luc-transfected cultured ARPE-19 cells was increased by ~5-fold after 4 days of culture (Fig. 1D). The enzymatic activities of AChE and TYR of cultured ARPE-19 cells were compared with that of A375 human melanoma cells. ARPE-19 cells showed higher TYR activity but weaker AChE activity when compared to A375 human melanoma cells (Fig. 1E and F). The protein expressions of AChE, BChE and ChAT were parallel to that of their transcripts (Fig. 1G left and right panels & Supplementary Fig. 3). Besides, the anti-AChE antibody
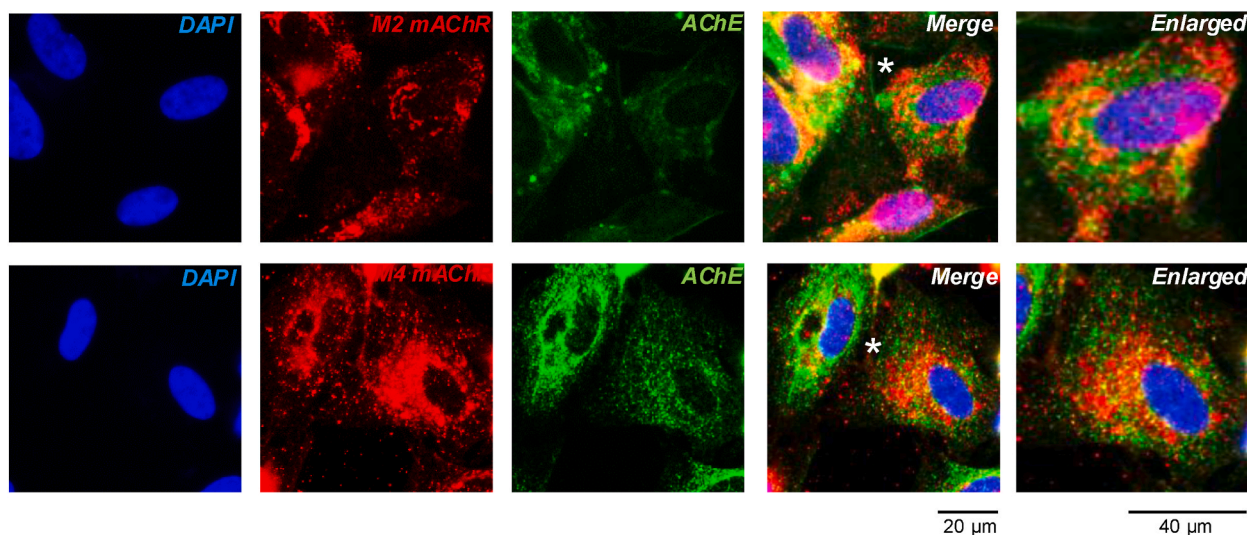
Fig. 8. Immunostainings of M2 and M4 mAChRs in cultured ARPE-19 cells. Cultured ARPE-19 cells were fixed with 4 % PFA for 15 min in room temperature and followed by staining of anti-M2 mAChR (red), anti-M4 mAChR (red), anti-AChE (green) in ARPE-19 cells with permeabilization with 0.1 % Triton X-100. Nucleus were stained with DAPI, $n = 4$.

stained the RPE cells robustly (Fig. 1H).

The expressions of melanogenic molecules in cultured ARPE-19 cells were determined. The mRNAs encoding TYR and MITF were significantly increased on day 4 (~8.3-fold and ~13-fold) (Fig. 2A). Besides, TRP1 mRNA was greatly increased on day 4 (~44-fold) (Fig. 2B). The luciferase activities driven by the promoters, pTYR-Luc and pMITF-Luc, in the transfected cultured ARPE-19 cells were increased in time-dependent manners (Fig. 2C). In parallel, the protein expressions of TYR, TRP1 and MITF were upregulated during the culture, similar to their transcripts (Fig. 2E upper and lower panels &Supplementary Fig. 4). The highest content of melanin in ARPE-19 cells during the culture was starting on day 3 (~130 % of increase) (Fig. 2D). Immunostainings of anti-TYR and anti-RPE65 indicated the distinct characteristics of RPE (Fig. 2F).

3.2. cAMP and ACh upregulate melanogenesis

In cultured ARPE-19 cells, forskolin was administered to induce the level of intracellular cAMP. The results of Western blots showed that forskolin induced an upregulation of AChE, TYR and MITF in dose- and time-dependent manners (Fig. 3A&B upper and lower panels &Supplementary Fig. 5-6). The protein level of AChE was increased to a plateau at 10 μM of administered forskolin (~150 % of increase) up to 50 μM. The melanogenic proteins, such as TYR and MITF, were increased under forskolin application (Fig. 3A lower panel). Besides, the increases of these proteins were identified after 6 h of treating forskolin (Fig. 3B). The forskolin-induced expressions were also identified in mRNA level, and which were in dose-dependent manners (Fig. 3C). In parallel, the forskolin-induced expressions of AChE, TYR and MITF mRNAs were shown in time-dependent manners (Fig. 3D). In parallel, the enzymatic activities of AChE and TYR in the cultures were induced by applied forskolin. At 50 μM of forskolin, the induced AChE activity reached ~7-fold, and TYR activity was at ~4.6-fold (Fig. 3E). Moreover, the content of melanin was raised by ~120 % under 50 μM forskolin (Fig. 3F). In pAChE-Luc, pTYR-Luc, pMITF-Luc and pCRE-Luc transfected cultured ARPE-19 cells, the applications of forskolin induced the promoter activities in dose-dependent manners, and the inductions were robustly abolished by inclusion of H89 (a PKA inhibitor) (Fig. 4A–D).

Cultured ARPE-19 cells were treated with ACh, ranged from 0 to 100 μM, with or without tacrine (5 μM; an AChE inhibitor). The mRNA levels of AChE, TYR and MITF were upregulated in dose-dependent manners (Fig. 5A). The level of AChE mRNA was plateau at ~25 μM of ACh (~50 % of increase). In parallel, the levels of TYR and MITF mRNAs were increased, showing induction starting at about 25 μM ACh. The inclusion of tacrine robustly enhanced the induced effects of ACh in all cases (Fig. 5A). The protein levels of AChE, TYR and MITF were determined at different doses of applied ACh, with or without tacrine (Fig. 5B and **Supplementary** Fig. 7-8). In all scenarios, the quantification of proteins was in dose-dependent manners of applied ACh, i.e., AChE (Fig. 5C), TYP (Fig. 5D) and MITF (Fig. 5E), and which were enhanced by the presence of tacrine. Similar situation was revealed for the content of melanin in cultured ARPE-19 cells in responding to ACh and tacrine treatments (Fig. 5F). The robust effect of tacrine in MITF expression could be in two folds: (i) blocking AChE to increase ACh level; and (ii) acting directly onto MITF promoter. These notions have to be validated.

3.3. Muscarinic AChRs regulates melanogenesis

The ACh-induced effects were not blocked by nicotinic AChR antagonist (data not shown), as well as the inductive effect of forskolin. Therefore, we hypothesized that mAChRs could be the receptor responsible for such ACh response. Bethanechol (Bch), an

agonist for all mAChRs, was applied onto cultured ARPE-19 cells, which upregulated the enzymatic activities and mRNA levels of AChE and TYR, similar to that of applied ACh (Fig. 6A and B). The protein levels of AChE, TYR and MITF were robustly induced by Bch (Fig. 6C upper and lower panels &Supplementary Fig. 9). In addition, the promoter activities, driven by pAChE-Luc, pTYR-Luc, pMITF-Luc and pCRE-Luc, were induced robustly by Bch in the transfected ARPR-19 cells, again in dose-dependent manners (Fig. 6D and E). At 1 mM Bch, the inductive effects on the biomarker expressions had reached maximum in most cases. Lower dose of Bch from 0.2 to 0.8 mM were applied in similar studies, which showed much better dose-responsive curves in all scenarios (Supplementary Fig. 1 & Supplementary Fig. 10).

In order to identify specific mAChR for Bch-induced effects, specific antagonists of mAChRs were applied here in cultured ARPE-19 cultures. The Bch-induced enzymatic activities and mRNA levels of AChE, TYR and MITF, as well as the content of melanin, were fully blocked by gallamine (a M2 specific antagonist), tropicamide (a M4 specific antagonist) and atropine (non-specific antagonist for mAChRs). Pirenzepine (a M1 selective antagonist) together with 4-DAMP (a M3 selective antagonist) did not block the response (Fig. 7A and B). In the DNA transfected cultures, the Bch-induced promoter activities, driven by pAChR-Luc, pTYR-Luc, pMITF-Luc and pCRE-Luc, were fully blocked by gallamine, tropicamide and atropine, but not for pirenzepine and 4-DAMP (Fig. 7C). Moreover, the Bch-induced enzymatic activities of AChE and TYR were, parallelly, blocked by gallamine, tropicamide and atropine (Fig. 7D). These pharmacological effects indicated the receptors responsible for ACh-dependent regulation of melanogenesis could be M2 and/or M4 mAChRs. Supporting this notion, cultured ARPE-19 cells were recognized by antibodies specific to M2 and M4 mAChRs (Fig. 8). The specificities of M2 and M4 staining were further verified in control immunostainings without the primary antibodies (Supplementary Fig. 2).

4. Discussion

Human pigment epithelia cells have been shown to express different cholinergic molecules, e.g., AChE and mAChR [23,24]. Here, we are proposing that melanogenesis in ARPE-19 cells is being regulated via mAChRs, e.g., regulation of the amounts of TYR, MITF and melanin. The notion is supported by several lines of evidence, including (i) co-regulation of cholinergic molecules with melanogenic biomarkers during the growth of epithelia cells; (ii) induced expressions of cholinergic and melanogenic biomarkers by forskolin, and which was blocked by H89; and (iii) ACh/Bch in inducing the expressions of cholinergic and melanogenic biomarkers, and which was specifically blocked by M2/M4 antagonists. The outcome of this event is an increased level of melanin in the pigment epithelia cells.

A close relationship of AChE and BChE in development of retina has been reported [25]. In chicken foetal RPE, AChE and BChE activities were identified during early development of retina [26]. AChE activity of chicken RPE was increased during the embryonic stage (embryonic age 5–20) and decreased after hatching. Meanwhile, BChE activity was decreased during the same period. Similar observation was revealed in cultured RPE cells from chicken embryos [27], suggesting AChE and BChE may have roles in the melanogenesis. In addition, the expression of AChE in ARPE-19 cells was proposed to be involved in the hydrogen peroxide-induced apoptosis [24]. In line to cAMP-dependent pathway in melanogenesis of skin, *klotho*, an aging-suppressor gene coded protein [28], was shown to alleviate cAMP signalling and to induce the process of melanogenesis of ARPR-19 cells [29]. In parallel, ~30 % of lesser melanin was revealed in RPE of the *klotho* knocked out mice (*klotho$^{-/-}$*) [30]. These findings could be attributed to activation of cAMP-dependent pathway, similar to pharmacological effects of forskolin [31–33]. On the other hand, Bt$_2$-cAMP has been shown to upregulate the melanogenesis in murine melanoma cell line, B16F10 cells: the cause was triggered by the induced TYR expression, as such showing an increased melanin content [14].

Where is the source of ACh in triggering the aforementioned cholinergic events? The photoreceptor outer segments express ChAT and high affinity choline transporter, which therefore can release ACh to adjacent RPE cells, serving as a communication between photoreceptors and RPE cells [34]. Whether RPE cells, or other cell types, in vicinity producing ACh could be another possible source of ACh. Nevertheless, the ACh secretory cells in the retina need to be validated. In mammal, RPE expresses multiple subtypes of nAChRs [34–36] and mAChRs [23], and the ACh-induced events here could be mainly attributed by activation of M2 and M4 mAChRs. Both M2 and M4 mAChRs are G-protein coupled receptors, specifically having the signaling of G$_{i/o}$ protein [37]. Stimulation of M2 and M4 receptors was reported to decrease intracellular cAMP by inhibiting adenylate cyclase [38]. Nevertheless, our results were in line with Michal et al. [39,40], where the stimulation of M2 mAChR could upregulate intracellular cAMP in the receptor expressing Chinese hamster ovary cells. Thus, ARPE-19 cells could exhibit similar conditions leading to this result of increased cAMP.

The mechanism of melanogenesis in adult RPE cells remained unclear [4]. This question was raised because RPE cells were reported to be post-mitotic after birth, where the turnover of RPE cells was very limited [41]. In a RPE cell atrophy model, the cell numbers of RPE were returned to nearly the healthy level after weeks of post-induction of atrophy [42]. This indicated that adult RPE cells may have the potential to regulate melanogenesis during the cell division, and possibility which could be mediated by the cAMP-dependent pathway, as proposed here. The non-neuronal function of ACh, as well as that of M2 and M4 mAChRs, in regulating the melanogenesis process in ARPE-19 cells could be a key stage of retinal function and development. Mouse models having RPE damage [43] could be used as AMD model in testing the role of ACh. These findings provide a new insight into the prevention of early AMD onset that primarily occurs in aged patients.

Data availability statement

The data that support the findings of this study are available on request from the corresponding author.

CRediT authorship contribution statement

Ivan Kong: Writing – review & editing, Writing – original draft, Investigation, Formal analysis, Conceptualization. **Gary Ka-Wing Yuen:** Visualization, Methodology, Conceptualization. **Qi-Yun Wu:** Methodology, Conceptualization. **Maggie Sui-Sui Guo:** Methodology, Conceptualization. **Jin Gao:** Methodology. **Tina Ting-Xia Dong:** Resources. **Karl Wah-Keung Tsim:** Writing – review & editing, Writing – original draft, Project administration, Funding acquisition, Conceptualization.

Declaration of competing interest

The authors declare that they have no known competing financial interests or personal relationships that could have appeared to influence the work reported in this paper.

Acknowledgements

Appendix A. Supplementary data

Supplementary data to this article can be found online at https://doi.org/10.1016/j.heliyon.2024.e36207.

References

[1] S. Yang, J. Zhou, D. Li, Functions and diseases of the retinal pigment epithelium, Front. Pharmacol. 12 (1) (2021), https://doi.org/10.3389/fphar.2021.727870.
[2] A. Lakkaraju, A. Umapathy, L.X. Tan, et al., The cell biology of the retinal pigment epithelium, Prog. Retin. Eye Res. (2020) 100846, https://doi.org/10.1016/j.preteyeres.2020.100846.
[3] S. Peters, U. Schraermeyer, Characteristics and functions of melanin in retinal pigment epithelium, Ophthalmologe 98 (12) (2001) 1181–1185, https://doi.org/10.1007/s00347017001.
[4] U. Schraermeyer, Does melanin turnover occur in the eyes of adult vertebrates? Pigm. Cell Res. 6 (4) (1993) 193–204, https://doi.org/10.1007/s003470170011.
[5] A. Biesemeier, F. Kreppel, S. Kochanek, et al., The classical pathway of melanogenesis is not essential for melanin synthesis in the adult retinal pigment epithelium, Cell Tissue Res. 339 (3) (2010) 551–560, https://doi.org/10.1007/s00441-009-0920-9.
[6] F.L. Ferris, S.L. Fine, L. Hyman, Age-related macular degeneration and blindness due to neovascular maculopathy, Arch. Ophthalmol. 102 (11) (1984) 1640–1642, https://doi.org/10.1001/archopht.1984.01040031330019.
[7] R.A. Bone, B. Brener, J.C. Gibert, Macular pigment, photopigments, and melanin: distributions in young subjects determined by four-wavelength reflectometry, Vision Res 47 (26) (2007) 3259–3268, https://doi.org/10.1016/j.visres.2007.09.002.
[8] P.U. Dugel, C.N. Zimmer, Imaging of melanin disruption in age-related macular degeneration using multispectral imaging, Ophthalmic Surg Lasers Imaging Retina 47 (2) (2016) 134–141, https://doi.org/10.3928/23258160-20160126-06.
[9] A. Stahl, The diagnosis and treatment of age-related macular degeneration, Dtsch Arztebl Int 117 (29) (2020) 513–520, https://doi.org/10.3238/arztebl.2020.0513.
[10] Y.-S. Kwon, M. Zheng, A.Y. Zhang, et al., Melanin-like nanoparticles as an alternative to natural melanin in retinal pigment epithelium cells and their therapeutic effects against age-related macular degeneration, ACS Nano 16 (11) (2022) 19412–19422, https://doi.org/10.1021/acsnano.2c09087.
[11] S.M. Yacout, K.L. McIlwain, S.P. Mirza, et al., Characterization of retinal pigment epithelial melanin and degraded synthetic melanin using mass spectrometry and *in vitro* biochemical diagnostics, Photochem. Photobiol. 95 (1) (2019) 183–191, https://doi.org/10.1111/php.12934.
[12] M. Cichorek, M. Wachulska, A. Stasiewicz, et al., Skin melanocytes: biology and development, Postepy Dermatol Alergol 30 (1) (2013) 30–41, https://doi.org/10.5114/pdia.2013.33376.
[13] M.A. Maranduca, D. Branisteanu, D.N. Serban, et al., Synthesis and physiological implications of melanic pigments, Oncol. Lett. 17 (5) (2019) 4183–4187, https://doi.org/10.3892/ol.2019.10071.
[14] Q. Wu, A.H.Y. Fung, M.L. Xu, et al., Microphthalmia-associated transcription factor up-regulates acetylcholinesterase expression during melanogenesis of murine melanoma cells, J. Biol. Chem. 293 (37) (2018) 14417–14428, https://doi.org/10.1074/jbc.RA118.003729.
[15] G. Hunt, C. Todd, J.E. Cresswell, et al., Alpha-melanocyte stimulating hormone and its analogue Nle4DPhe7 alpha-MSH affect morphology, tyrosinase activity and melanogenesis in cultured human melanocytes, J. Cell Sci. 107 (Pt 1) (1994) 205–211, https://doi.org/10.1242/jcs.107.1.205.
[16] T.A. Luger, T. Scholzen, S. Grabbe, The role of alpha-melanocyte-stimulating hormone in cutaneous biology, J. Invest. Dermatol. Symp. Proc. 2 (1) (1997) 87–93, https://doi.org/10.1038/jidsymp.1997.17.
[17] S.A. Grando, M.V. Dahl, Activation of keratinocyte muscarinic acetylcholine receptors reverses pemphigus acantholysis, J. Eur. Acad. Dermatol. Venereol. 2 (4) (1993) 72–86, https://doi.org/10.1111/j.1468-3083.1993.tb00016.x.
[18] S.A. Grando, Biological functions of keratinocyte cholinergic receptors, J. Invest. Dermatol. Symp. Proc. 2 (1) (1997) 41–48, https://doi.org/10.1038/jidsymp.1997.10.
[19] A. Ndoye, R. Buchli, B. Greenberg, et al., Identification and mapping of keratinocyte muscarinic acetylcholine receptor subtypes in human epidermis, J. Invest. Dermatol. 111 (3) (1998) 410–416, https://doi.org/10.1046/j.1523-1747.1998.00299.x.
[20] G.L. Ellman, K.D. Courtney, V. Andres, et al., A new and rapid colorimetric determination of acetylcholinesterase activity, Biochem. Pharmacol. 7 (2) (1961) 88–95, https://doi.org/10.1016/0006-2952(61)90145-9.

[21] K.W. Tsim, W.R. Randall, E.A. Barnard, An asymmetric form of muscle acetylcholinesterase contains three subunit types and two enzymic activities in one molecule, Proc Natl Acad Sci U S A. 85 (4) (1988) 1262–1266, https://doi.org/10.1073/pnas.85.4.1262.

[22] N.L. Siow, R.C.Y. Choi, K.W.K. Tsim, et al., A cyclic AMP-dependent pathway regulates the expression of acetylcholinesterase during myogenic differentiation of C2C12 cells, J. Biol. Chem. 277 (39) (2002) 36129–36136, https://doi.org/10.1074/jbc.M206498200.

[23] X. Zhou, D. Yan, J. Qu, et al., Expression of muscarinic acetylcholine receptor–1 in human retinal pigment epithelium, Invest. Ophthalmol. Vis. Sci. 47 (13) (2006) 881.

[24] L. Cai, H.-F. Liao, X.-J. Zhang, et al., Acetylcholinesterase function in apoptotic retina pigment epithelial cells induced by H2O2, Int. J. Ophthalmol. 6 (6) (2013) 772–777, https://doi.org/10.3980/j.issn.2222-3959.2013.06.06.

[25] P.G. Layer, R. Alber, O. Sporns, Quantitative development and molecular forms of acetyl-and butyrylcholinesterase during morphogenesis and synaptogenesis of chick brain and retina, J. Neurochem. 49 (1) (1987) 175–182, https://doi.org/10.1111/j.1471-4159.1987.tb03411.x.

[26] R. Salceda, M.T. Martinez, Characterization of acetylcholinesterase and butyrylcholinesterase activities in retinal chick pigment epithelium during development, Exp. Eye Res. 54 (1) (1992) 17–22, https://doi.org/10.1016/0014-4835(92)90064-Y.

[27] R. Salceda, G. Sanchez, J. León-Cázares, Characterization of cholinesterase activities in primary cultures of retinal pigment epithelium, Invest. Ophthalmol. Vis. Sci. 33 (5) (1992) 1690–1695. https://iovs.arvojournals.org/article.aspx?articleid=2161150.

[28] M. Kuro-o, Y. Matsumura, H. Aizawa, et al., Mutation of the mouse klotho gene leads to a syndrome resembling ageing, Nature 390 (6655) (1997) 45–51, https://doi.org/10.1038/36285.

[29] J. Yang, N. Matsukawa, H. Rakugi, et al., Upregulation of cAMP is a new functional signal pathway of Klotho in endothelial cells, Biochem Biophys Res Commu 301 (2) (2003) 424–429, https://doi.org/10.1016/S0006-291X(02)03056-5.

[30] M. Kokkinaki, M. Abu-Asab, N. Gunawardena, et al., Klotho regulates retinal pigment epithelial functions and protects against oxidative stress, J. Neurosci. 33 (41) (2013) 16346–16359, https://doi.org/10.1523/JNEUROSCI.0402-13.2013.

[31] P.K. Wagoner, B.S. Pallotta, Modulation of acetylcholine receptor desensitization by forskolin is independent of cAMP, Science 240 (4859) (1988) 1655–1657, https://doi.org/10.1126/science.2454507.

[32] P.A. Insel, R.S. Ostrom, Forskolin as a tool for examining adenylyl cyclase expression, regulation, and G protein signalling, Cell. Mol. Neurobiol. 23 (3) (2003) 305–314, https://doi.org/10.1023/A:1023684503883.

[33] Q. Wang, X. Su, R. Zhu, et al., cAMP agonist forskolin disrupts mitochondrial metabolism and induces senescence in human mesenchymal cells, Stem Cells Dev. 32 (3) (2023) 87–98, https://doi.org/10.1089/scd.2022.0180.

[34] H. Matsumoto, K. Shibasaki, M. Uchigashima, et al., Localization of acetylcholine-related molecules in the retina: implication of the communication from photoreceptor to retinal pigment epithelium, PLoS One 7 (8) (2012) e42841, https://doi.org/10.1371/journal.pone.0042841.

[35] X.-Y. Zhang, T.K. Ng, M.E. Brelén, et al., Disruption of retinal pigment epithelial cell properties under the exposure of cotinine, Sci. Rep. 7 (1) (2017) 3139, https://doi.org/10.1038/s41598-017-03283-x.

[36] V. Maneu, G. Gerona, L. Fernández, et al., Evidence of alpha 7 nicotinic acetylcholine receptor expression in retinal pigment epithelial cells, Vis. Neurosci. 27 (5) (2010) 139–147, https://doi.org/10.1017/S0952523810000246.

[37] K. Qin, C. Dong, G. Wu, et al., Inactive-state preassembly of Gq-coupled receptors and Gq heterotrimers, Nat. Chem. Biol. 7 (10) (2011) 740–747, https://doi.org/10.1038/nchembio.642.

[38] S.L. Miller, H.H. Yeh, Chapter 3 - neurotransmitters and neurotransmission in the developing and adult nervous system, in: P.M. Conn (Ed.), Conn's Transl Neuro, 2017, pp. 49–84, https://doi.org/10.1016/B978-0-12-802381-5.00004-X.

[39] P. Michal, M. Lysíková, S. Tucek, Dual effects of muscarinic M(2) acetylcholine receptors on the synthesis of cyclic AMP in CHO cells: dependence on time, receptor density and receptor agonists, Br. J. Pharmacol. 132 (6) (2001) 1217–1228, https://doi.org/10.1038/sj.bjp.0703931.

[40] P. Michal, E.E. El-Fakahany, V. Dolezal, Muscarinic M2 receptors directly activate Gq/11 and Gs G-proteins, J Pharmacol Exp Ther 320 (2) (2007) 607–614, https://doi.org/10.1124/jpet.106.114314.

[41] H. Gao, J.G. Hollyfield, Aging of the human retina. Differential loss of neurons and retinal pigment epithelial cells, Invest. Ophthalmol. Vis. Sci. 33 (1) (1992) 1–17.

[42] M. Chen, D. Rajapakse, M. Fraczek, et al., Retinal pigment epithelial cell multinucleation in the aging eye – a mechanism to repair damage and maintain homoeostasis, Aging Cell 15 (3) (2016) 436–445, https://doi.org/10.1111/acel.12447.

[43] N. Zhang, X. Zhang, P.E. Girardot, et al., Electrophysiologic and morphologic strain differences in a low-dose NaIO3-induced retinal pigment epithelium damage model, Transl Vis Sci Technol 10 (8) (2021) 10, https://doi.org/10.1167/tvst.10.8.10.